ELSEVIER

Contents lists available at ScienceDirect

Journal of Luminescence

journal homepage: www.elsevier.com/locate/jlumin



Full Length Article

Investigation of the role of iron doping on the structural, optical and photoluminescence properties of sol–gel derived TiO₂ nanoparticles



Shahid Husain ^{a,*}, Lila A. Alkhtaby ^b, Emilia Giorgetti ^c, Angela Zoppi ^c, Maurizio Muniz Miranda ^d

- ^a Department of Physics, Aligarh Muslim University, Aligarh 202002, India
- ^b Department of Physics, King Abdulaziz University, Jeddah, Saudi arabia
- ^c Istituto dei Sestemi Complessi ISC-CNR Sezione di Firenze, Seso Florentino, 50019 Firenze, Italy
- ^d Department of Chemistry, University of Firenze, Seso Florentino, 50019 Firenze, Italy

ARTICLE INFO

Article history: Received 3 March 2015 Received in revised form 9 November 2015 Accepted 2 December 2015 Available online 11 December 2015

Keywords: Titania Sol-gel process Raman spectroscopy Photoluminescence

ABSTRACT

We have synthesized the Fe doped titania (TiO_2) nanopowders using sol–gel process. These samples are formed in anatase form of titania as revealed by X-ray diffraction patterns. The UV/Vis absorption spectra exhibit that Fe-doping causes a considerable red shift of the absorption edge. Energy bandgap estimated using Tauc's relation is found be of direct transition nature and Fe doping decreases the bandgap significantly. Raman spectra indicate an anatase structure of tetragonal crystal symmetry that belongs to the space group D_{4h}^{19} . Photoluminescence spectra recorded in ultraviolet and visible regions reveal that Fe doping increases the photocatalytic activity of our samples. FTIR spectra show that characteristic Ti–O band is observed around 680 cm $^{-1}$ for pure TiO₂ sample and on iron doping it shifted to 592 cm $^{-1}$.

© 2015 Elsevier B.V. All rights reserved.

1. Introduction

Titanium dioxide (TiO2) is a wide-band gap semiconductor used in solar and chemical processes that has emerged as an excellent material for environmental purification [1,2]. Titanium dioxide is an n-type semiconductor with electrons as the majority carriers and exists in three different polymorphic phases: anatase, rutile, and brookite. Anatase and rutile are the most common polymorphs that crystallize in a tetragonal lattice and their structure is described in chains of TiO₆ octahedra with different physical and chemical behavior [3,4]. TiO₂ is non-toxic, chemically stable and low cost material that has a positive impact on the environment. It has attracted more attention in environmental studies and applications due to its applicability to the treatment of pollutants and waste using photocatalysis. The titanium dioxide (TiO₂) photocatalyst is being widely studied for air and water purification applications and has emerged as an excellent photocatalytic material for environmental purification because of its high stability, low cost, non toxicity, high oxidation potential and chemically favorable properties. However, it only utilizes the UV

portion of the solar spectrum as an energy source (less than 4% of the total sunlight energy). This behavior is due to its high band gap value of 3.2 eV. The modification of light harvesting properties of TiO_2 by doping has become an important research topic to achieve an efficient operation range under UV and visible light.

Iron is frequently employed owing to its unique half-filled electronic configuration, which might narrow the energy gap through the formation of new impurity energy levels [5]. We have synthesized the doped the iron doped in TiO₂ using sol–gel process and investigated its structural, optical and luminescence properties to observe the effect of iron doping on these properties.

2. Experimental

Iron doped titanium dioxide $(Ti_{1-x}Fe_xO_2)$ samples have been prepared by sol–gel process. The precursors were $Fe(NO_3)_3$, titanium tetra-isopropoxide (TTIP), ethanol and distilled water. In the synthesis process we have taken 4 ml of TTIP with 40 ml of ethanol and dissolved it in 50 ml distilled water at room temperature. This solution is called as solution A. The other solution B is prepared by dissolving 5 ml of $Fe(NO_3)_2$ in a 0.4 M ethanolic solution and distilled water. The solution B is added drop wise to

^{*} Corresponding author. Tel.: +919719006563 E-mail address: s.husain@lycos.com (S. Husain).

the solution A, under vigorous stirring for 30 min at room temperature. The resulted gels are kept in an oven at 150 °C to remove the moisture until the dry mixture is obtained. Finally, the samples were ground and calcinated at 400 °C for 2 h. The X-ray diffraction patterns of samples are recorded by Rigaku MiniFlex X-ray diffractometer in the 2θ range of 20–80°. This diffractometer has the minimum step width of 0.005° with an accuracy of $\pm 0.02^{\circ}$. The morphology is investigated with scanning electron microscope (Quanta FEG450). UV/Vis spectra are recorded using a Varian Cary-5 spectrophotometer with a wavelength range of 180-3300 nm and resolution of 0.05 nm. We have recorded the Raman spectra using a Renishaw RM2000 micro Raman apparatus equipped with a diode laser emitting at 785 nm. The backscattered Raman signals were filtered by a double holographic Notch filter system and detected by an air cooled CCD. Acquisition time was varying from 5–30 s. The resolution of this instrument is 3 cm⁻¹. We have utilized the Perkin-Elmer LS55 spectrophotometer equipped with a high energy pulsed Xenon source with a slit of width 10 nm and resolution of 0.1 nm to record the photoluminescence. Brucker Tensor-37 FTIR spectrometer is used to record the FTIR spectra in transmission mode. This spectrometer has a resolution of 0.3 cm^{-1} .

3. Results and discussion

3.1. Structural and morphological analysis

X-ray diffraction patterns of $\mathrm{Ti}_{1-x}\mathrm{Fe}_x\mathrm{O}_2$ (x=0.01, 0.02, 0.03 and 0.05) samples are shown in Fig. 1. The anatase structure was confirmed by indexing the diffraction peaks with most intense peak at 2θ =24.5° corresponding to the plane (101). It could be assumed that Fe^{3+} ions are most likely substituted in Ti^{4+} sites within TiO_2 because the ionic radius of Fe^{3+} ions (0.64 Å) is similar to Ti^{4+} ions (0.68 Å). The unit cell volume is calculated using the relation: $V=a^2c$ where a=b, c are lattice parameters. The lattice parameters, unit cell volume and crystallite size calculated with Sherrer equation using most intense peak (101), are tabulated in Table 1 for all the Fe doped samples. These values are in good agreement with earlier reports [6–9]. Fig. 2 shows the scanning electron microscope (SEM) images of sol–gel synthesized $\mathrm{Ti}_{1-x}\mathrm{Fe}_x\mathrm{O}_2$ (x=0.01, 0.02, 0.03 and 0.05) samples. These images

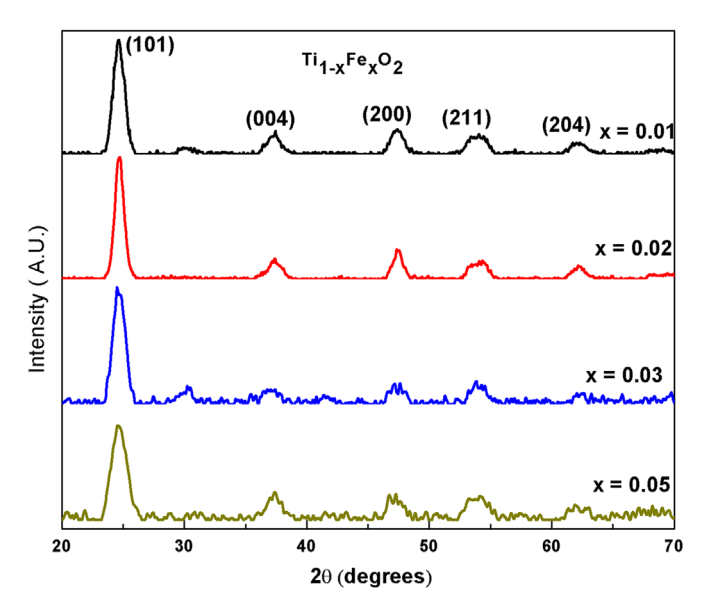


Fig. 1. The powder X-ray diffraction patterns of $\text{Ti}_{1-x}\text{Fe}_x\text{O}_2(x=0.01, 0.02, 0.03 \text{ and } 0.05)$ recorded at room temperature.

reveal that the as-grown nanoparticles are almost spherical in size with average particle size in the range of 35–50 nm. Our results are in good agreement with other reports [6,7] on these materials.

3.2. Raman spectroscopic analysis

In order to investigate the influence of Fe doping on microstructure and vibrational properties, Raman scattering experiments were carried out. Raman scattering is a versatile technique for detecting the incorporation of dopants and the resulted defects and lattice disorder in the host lattice The Raman spectra of Fe doped TiO₂ are recorded at room temperature for different concentrations as shown in Fig. 3. Raman spectra indicate an anatase structure of tetragonal crystal symmetry that belong to the space group D_{4h}^{19} , with two body center unit cells one with $A_{2u}+2B_{1g}+3E_{g}$ Raman active modes the other cell with $A_{2u}+2E_{g}$ infra-red active mode [10]. Our pure and Fe doped TiO₂ samples show Raman active modes appearing at 248-250, 323, 364, 395-399, 516 and 639-641 cm⁻¹ characterizing the absorption of anatase TiO_2 [9] as shown in Fig. 3. The band at 641 cm⁻¹ is assigned/related to the $E_{\rm g}$ mode, the mode at $516\,{\rm cm}^{-1}$ is a doublet of A_{1g} and B_{1g} . The weak bands appearing at 323 and 364 cm⁻¹ for 2% and 3% doping concentrations may be related to the Fe clusters [11] or to the FeTiO₃ phase [12,13]. We have not observed the characteristic peaks of Fe₂O₃ in our spectra. The line width (FWHM) broadening can be clearly seen with the increase in the concentration of Fe content that may be due to the decrease in the crystallite size. We have summarized all the observed Raman bands for different concentrations of iron in Table 2.

3.3. UV/Vis spectroscopy

UV/Vis spectra were recorded for ${\rm Ti_{1-x}Fe_xO_2}$ (x=0.01, 0.02, 0.03 and 0.05) as shown in Fig. 4. We have recorded the absorption spectra of the samples after dilution in de-ionized water and sonification. The absorption spectra show that Fe-doping causes a considerable red shift of the absorption edge. This is consistent with the work of Kokila et al. [6].

The optical band gap (E_g) is defined as the energy where the absorption coefficient has a value $> 10^4 \ cm^{-1}$. It can be calculated using the Tauc relation [14] as

$$\alpha h \upsilon = A(h \upsilon - Eg)^{m}$$
.

where α is absorption coefficient given by α =2.303 log (T/d) (d is the length of cuvette in which sample is filled and T is the transmittance), hv is the photon energy. The value of exponent depends on nature of bandgap. It will be equal to ½ for direct bandgap and has the value 2 for indirect bandgap. The values of E_g can be determined by taking the intercept of the extrapolation to zero absorption with photon energy axis i.e. $(\alpha hv)^2 \rightarrow 0$.

Generally, anatase TiO_2 has an indirect band gap but in literature there are reports that suggest that anatase TiO_2 exist with direct band gap in case of nano form. In view of this, in order to investigate the nature and to determine the value of the band gap, we have fitted our absorption data using Tauc's relation for both indirect and direct band gap transitions. Fig. 5 shows the $(\alpha h \nu)^{1/2}$ versus energy plots (indirect transition) for iron doped TiO_2 samples. Fig. 6(a) and (b) show the $(\alpha h \nu)^2$ versus energy plots(direct transition) for pure TiO_2 and iron doped samples. The plots shown in Fig. 5 yield no meaningful results. Our data fits to the direct band gap relation as shown in Fig. 6(a) and (b). In case of pure TiO_2 the band gap is found to be 3.10 eV and with the iron doping a decrease is observed in the band gap. The values of band gap for different concentrations of iron are tabulated in Table 1.

Download English Version:

https://daneshyari.com/en/article/5398649

Download Persian Version:

https://daneshyari.com/article/5398649

<u>Daneshyari.com</u>